

Magnetization and magneto-electric effect in La-doped BiFeO₃

G. Le Bras-Jasmin, D. Colson, A. Forget, N. Genand-Riondet, P. Bonville

CEA, Centre d'Etudes de Saclay, Service de Physique de l'Etat Condensé
91191 Gif-sur-Yvette, France

Abstract

We report on magnetisation and magnetocapacitance measurements in the multiferroic series Bi_{1-x}La_xFeO₃ for $0 \leq x \leq 0.25$. We show that doping with La reduces the threshold magnetic field for cancelling the magnetic spiral phase present in BiFeO₃, the effect being the strongest for $x=0.15$, which is the highest concentration for maintaining the non-centrosymmetric rhomboedral structure of BiFeO₃. Measurements of the dielectric constant as a function of magnetic field in the series also show a maximum magnetocapacitance for $x=0.15$. The results are interpreted within a model using a Landau development of the free energy up to 3rd order in the fields.

PACS numbers: 75.80.+q, 75.50.Ee, 77.22.Ch, 77.84.Bw

INTRODUCTION

Recently, the perovskite compound BiFeO₃, where ferroelectricity ($T_C = 850^\circ\text{C}$) and antiferromagnetism ($T_N = 370^\circ\text{C}$) coexist at room temperature, has been the subject of renewed interest^{1,2}. Such multiferroic^{3,4} materials can present a strong coupling between the electric and magnetic order parameters, also called the magnetoelectric (ME) effect. Thus they are potential candidates for applications to devices where, for instance, the magnetisation could be switched by the reversal of an electric field⁵. However, this is possible if some net magnetisation arises in the material. In BiFeO₃, the antiferromagnetic (AF) structure is of G-type, but it is inhomogeneous, showing a spiral cycloidal spin arrangement in which the Fe³⁺ moments rotate in a plane, with an incommensurate period $\lambda \sim 620\text{\AA}$ ^{6,7}. Due to the magnetoelectric coupling, the two Fe³⁺ sublattices are canted, resulting in a weak local net magnetisation, which however averages to zero over a period of the incommensurate modulated spin structure¹. So the macroscopic magnetization is cancelled in BiFeO₃. Another consequence of the cycloidal spin structure is that it inhibits the observation of the linear ME effect⁸, i.e. of the linear dependence of the induced electric polarisation on the magnetic field. The ME coupling is however strong enough to allow the reversal of AF domains by switching the electric field, as shown recently⁹.

It is therefore of interest to try and destroy the space-modulated spin cycloid. Various methods have been used for this purpose. The application of a high magnetic field, of the order of 20T, has been shown to induce a transition to a homogeneous AF state and to restore a non-zero magnetisation^{10,11}. Making BiFeO₃ in thin film form also leads to a homogeneous AF spin structure¹¹. Low level substitutions of rare earth ions (La, Dy, ...) for bismuth have an interesting effect: the introduction of rare earth cations in the rhombohedrally distorted structure of BiFeO₃ seems to increase the magnetocrystalline anisotropy¹², thus making the cycloidal spin structure energetically unfavourable. It can then be destroyed by a magnetic field lower than in pure BiFeO₃.

The La doped BiFeO₃ series has already been the subject of a certain number of investigations^{13,14,15,16,17}, but no systematic study as a function of the magnetic field was performed. Here, we determine the effect of a magnetic field up to 14T on the magnetisation

and dielectric constant (or magnetocapacitance) in the $\text{Bi}_{1-x}\text{La}_x\text{FeO}_3$ series, with x varying between 0 and 0.25. Our samples are polycrystalline powders or sintered pellets, whose crystal structure was determined as a function of x using X-ray diffraction. We show that the critical field for the transition from spiral to AF collinear magnetic structure decreases with increasing La doping, and we observe a correlated behaviour for the magnetocapacitance as a function of magnetic field.

CRYSTAL STRUCTURE AND EXPERIMENTAL DETAILS

Ceramic samples of $\text{Bi}_{1-x}\text{La}_x\text{FeO}_3$ ($0, 0.05, 0.10, 0.15, 0.17, 0.20$ and 0.25) were synthesized by a conventional solid state reaction using the starting oxides Bi_2O_3 , La_2O_3 and Fe_2O_3 (purity $\geq 99.99\%$). The mixtures were ground and calcined at 960°C during 10h. Then the samples were ground and pressed at 6 kbars into pellets with the dimensions of 5 mm in diameter and 1.5 mm in height and heated at 960°C for 10 hours to ensure the sintering of the samples. The samples were ground and analysed by powder X-ray diffraction to control their purity and to monitor the pattern evolution with La doping. XRD patterns were recorded on a D8 Advance diffractometer of Bruker-axs in θ - θ geometry using $\text{CuK}\alpha$ radiation and a ‘‘Sol-X’’ dispersive energy detector between 20° and 70° every 0.02° with a counting time of 20 seconds per step.

All the sintered samples were found single phase except for a small amount (~ 2 – 3%) of $\text{Bi}_{25}\text{FeO}_{39}$ which was detected in the samples with $x=0$ and $x=0.25$. The analysis of the XRD patterns shown in Figure 1 reveals some changes when increasing the La content, indicating structural modifications: the lattice symmetry gradually goes from rhombohedral (R3c) to orthorhombic (C222). For instance, the intensity of the (006) and (018) peaks becomes weaker and the splitting of the peaks around 39° and 50° decreases (see resp. insets (a) and (b) in Fig.1, where the splitting is shown by arrows), indicating that the rhombohedral distortion is reduced as the La content increases. The change from rhombohedral to orthorhombic symmetry is almost complete near $x=0.15$. These observations agree with those already published by Zalesskii et al.¹⁸. The reflections in the XRD pattern for the pure BiFeO_3 sample were indexed in a rhombohedral system (R3c) with lattice parameters $a=0.5576(2)$ nm and $c=1.3863(2)$ nm.

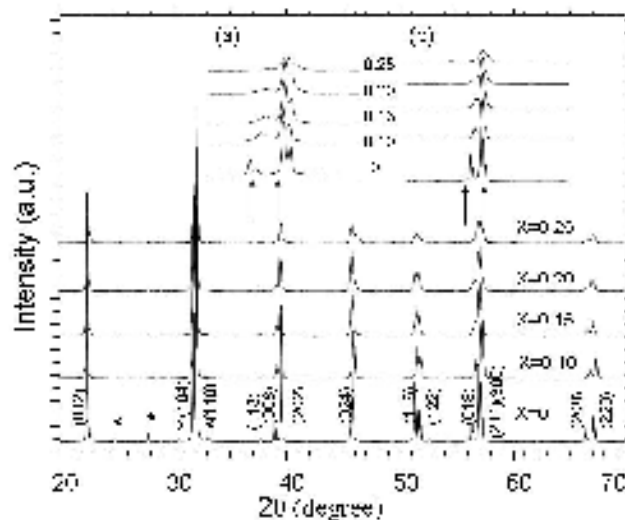


Figure 1: Powder X-Ray diffraction pattern in $\text{Bi}_{1-x}\text{La}_x\text{FeO}_3$ ($0 \leq x \leq 0.25$) at 300K using $\text{CuK}\alpha$ radiation. The asterisks correspond to the lines of the $\text{Bi}_{25}\text{FeO}_{39}$ impurity, especially visible for $x=0$. Insets: enlarged view near $2\theta = 39^\circ$ (a) and 50° (b) showing the progressive disappearance of the rhombohedral splitting (arrows) with increasing La content.

The isothermal dc magnetization curves were measured at 20 K as a function of the applied magnetic field H up to 14T, using an automated vibrating sample magnetometer (Cryogenic Limited VSM), on powder samples. It has been checked that the measurements are temperature independent up to 200K.

Dielectric constants were obtained by measuring the capacitance at 10 kHz on ceramic pellets (pressed at 6kbars) using a commercial LCR meter (Instek LCR-819). The sample size was typically 5 mm in diameter and 1.5 mm in thickness. Silver paste (Dupond 4929) painted on both planes was used as electrode. The magnetic field up to 8T was applied perpendicular to the plane of the disk. To avoid the ohmic losses due to grain boundaries, the measurements were not performed at room temperature, but at 100K where the capacitance is nearly T-independent with a value around 20 pF.

RESULTS

In the rhombohedrally distorted perovskite-type structure of BiFeO_3 , all the ions along the diagonal of the cube $[111]_c$ ($[001]_{\text{hex}}$) direction (iron and bismuth) are displaced relative to the ideal centrosymmetric positions, resulting below $T_C = 850^\circ\text{C}$ in a spontaneous electric polarization P_s along this axis, which will be labelled the z -axis in the following. The spiral magnetic structure is such that the Fe^{3+} moments lie in the $(110)_{\text{hex}}$ plane, the propagation vector being $\mathbf{q}_0 = [110]_{\text{hex}}$. Introducing the unit vectors $\mathbf{L} = (\mathbf{M}_1 - \mathbf{M}_2)/2M_0$ and $\mathbf{M} = (\mathbf{M}_1 + \mathbf{M}_2)/2M_0$, where \mathbf{M}_1 and \mathbf{M}_2 are the Fe^{3+} moments on the two AF sublattices and M_0 their common lengths, and following Ref.1, the magnetoelectric (ME) effect in BiFeO_3 results in the presence of energy invariants mixing electric and magnetic variables (see Fig.2), and leading thus to a coupling between them.

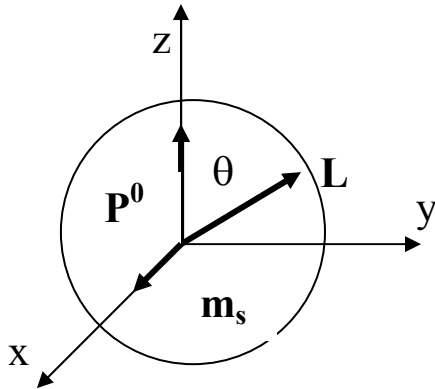


Figure 2: Schematic representation of the magnetic and electric polarisation vectors in BiFeO_3 . The magnetic spiral is taken to lie in the zOy plane, the angle θ determining the current position of the vector \mathbf{L} . \mathbf{P}^0 is the spontaneous electric polarisation along Oz .

The ME invariant of the type $g \propto P_z (H_y L_x - H_x L_y)$ leads to a spontaneous magnetic moment:

$$\mathbf{m}_s = -\partial g / \partial \mathbf{H} \propto P^0 (L_y, -L_x, 0) \propto P^0 \sin \theta \mathbf{i} \quad (1)$$

along the x -axis (see Fig.2). This spontaneous moment can be obtained in an equivalent manner considering the ME invariant:

$$g \propto P_z (M_y L_x - M_x L_y) = -\mathbf{P}^0 \cdot \mathbf{M} \times \mathbf{L} = -\mathbf{P}^0 \cdot \mathbf{M}_1 \times \mathbf{M}_2, \quad (2)$$

emphasizing thereby the similarity with the classical Dzyaloshinsky-Moriya interaction^{19,20}. Averaging over a period of the spiral, this moment vanishes. The ME invariant of the type:

$$g \propto E_z (M_y L_x - M_x L_y) \quad (3)$$

leads to a spontaneous polarisation:

$$\mathbf{P} = -\partial g / \partial \mathbf{E} \propto (M_y L_x - M_x L_y) \mathbf{k} \propto P^0 \sin^2 \theta \mathbf{k} \quad (4)$$

along the z -axis, which yields a slight modulation of the spontaneous polarisation along the spiral.

1) Magnetization measurements

In single crystal BiFeO_3 , the magnetization curve¹⁰ for fields up to 25T applied along $[001]_c$ shows an anomaly for a critical field $H_c = 20\text{T}$, with a weak ferromagnetic moment appearing for $H > H_c$. This has been attributed to the transition from the spiral magnetic structure to a canted collinear AF structure for $H > H_c$. In La-doped BiFeO_3 , the spiral structure has been shown to persist, in zero field, up to $x=0.10$ by nuclear (antiferro)magnetic resonance experiments¹⁸. From our experiments by ^{57}Fe Mössbauer spectroscopy, we could evidence the hallmark of the presence of the spiral structure, i.e. a characteristic spectral asymmetry²¹, only up to $x=0.05$. For higher dopings, the line broadenings due to cation disorder seem to preclude the observation of the spiral induced asymmetry. Thus the spiral magnetic structure is likely to be present as long as the crystal structure remains rhombohedral.

The isothermal magnetisation curves for various La doping contents $0 \leq x \leq 0.25$ in $\text{Bi}_{1-x}\text{La}_x\text{FeO}_3$ polycrystalline samples are shown in Fig. 3a. At low and intermediate fields,

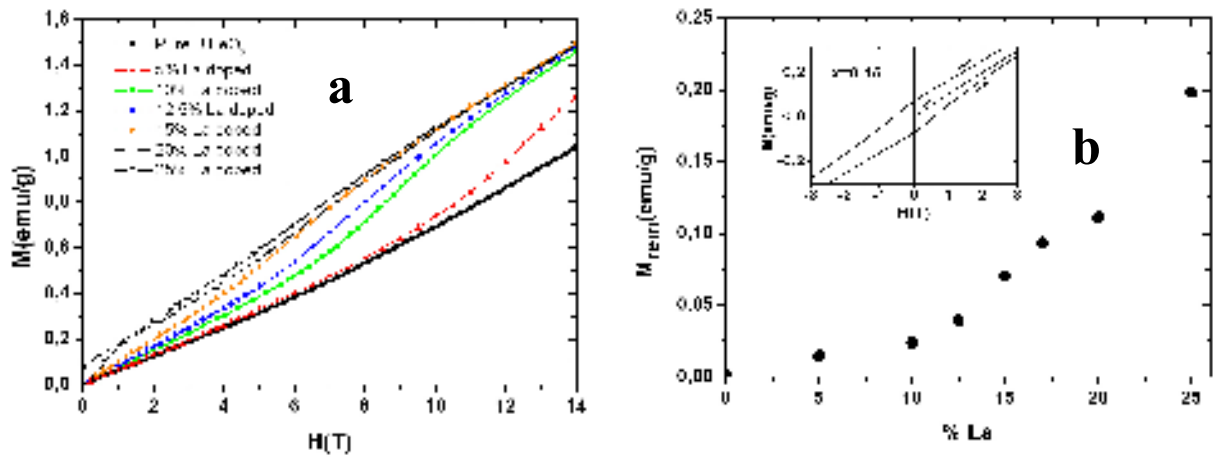


Figure 3: **a)** M - H response at 20K in $\text{Bi}_{1-x}\text{La}_x\text{FeO}_3$ ceramic samples for $0 \leq x \leq 0.25$. The lines are guide for the eyes; **b)** $H=0$ remanent magnetisation at 20K after increasing the field to 14T; insert: low field part of the hysteresis loop for $x=0.15$.

for pure BiFeO_3 , the $m(H)$ curve exhibits a linear dependence of the magnetization as a function of magnetic field, as expected for an antiferromagnetic spin structure. However, a slight departure from the linear behaviour appears for $H \sim 6\text{T}$, and for $H \geq 6\text{T}$ the field dependence is noticeably non linear. With increasing La content (up to $x=0.15$), the low field magnetization is still linear, but the field H_d for which the deviation from the linear behaviour is observed decreases. In samples with $x=0.10$, 0.125 and 0.15, one observes the recovery of a linear dependence, with a somewhat higher slope, at a higher field. For $x \geq 0.15$, extrapolation of the high field curve to $H=0$ yields a non-zero magnetisation of about 0.2 emu/g. For all doped samples, a small hysteresis is observed after increasing the field to 14T and back, the remanent magnetisation M_{rem} increasing with doping (see Fig.3b). This hysteresis is more pronounced for $x \geq 0.15$.

We interpret the overall behaviour of $m(H)$ for $x \leq 0.15$ as due to the crossover from the spiral magnetic structure to a collinear one when the field is increased. This crossover takes place for decreasing H_c as the La doping increases. The width of the transition (a few T) is due to the dependence of the critical field upon its orientation with respect to the crystal axes, leading to a spread of H_c values in our ceramic samples. In order to interpret more quantitatively the magnetisation curves, we computed the orientational dependence of the critical field H_c along the lines developed in Ref.1,2. For this purpose, one has to assume some spin configuration in the high field collinear phase, since there exists no experimental

determination of it. We make the reasonable assumption that, in the high field collinear phase, the \mathbf{L} vector is oriented perpendicular to the field and remains in the basal xOy plane. This implies that the anisotropy constant K must be taken negative. For a given orientation (ψ, γ) of the applied field, computation of the critical field is then straightforward and is given in detail in the Appendix. The parameters of the problem are the transverse AF susceptibility χ_{\perp} , the anisotropy density K , the gain in exchange energy density of the spiral phase $E_s = Aq_0^2$, where A is the exchange stiffness, and the ME-induced spontaneous magnetisation m_s . The critical field $H_c(\psi, \gamma)$ depends on m_s/χ_{\perp} and on $(Aq_0^2 - |K|/2)/\chi_{\perp}$. For a given applied magnetic field, we compute the powder magnetisation using:

$$M(H) = \frac{1}{4\pi} \int_0^{2\pi} d\gamma \int_0^{\pi} d\psi \sin \psi F(H, \psi, \gamma), \quad (5)$$

with:

$$\begin{aligned} F(H, \psi, \gamma) &= \frac{1}{2} \chi_{\perp} H (\sin^2 \psi \cos^2 \gamma + 1) \text{ for } H < H_c(\psi, \gamma), \\ F(H, \psi, \gamma) &= \chi_{\perp} H + m_s \sin \psi \text{ for } H > H_c(\psi, \gamma). \end{aligned} \quad (6)$$

The asymptotic forms for $m(H)$ after powder averaging are:

$$m(H) = 2/3 \chi_{\perp} H \text{ for } H < \min \{H_c(\psi, \gamma)\}, \quad (7)$$

i.e. in the spiral phase for all crystallites, with no ferromagnetic component as expected; and:

$$m(H) = \chi_{\perp} H + \pi/4 m_s \text{ for } H > \max \{H_c(\psi, \gamma)\}, \quad (8)$$

i.e. in the collinear phase for all crystallites. These expressions account for the increase of the $m(H)$ slope observed for the samples with $x=0.10$ and 0.125 between the low and high field regions; the model also predicts a weak ferromagnetic moment above the critical field, which is observed for the sample with $x=0.15$. The dependence of H_c on the anisotropy density K can be examined for instance in a simple case, i.e. when the field is applied along the x-axis. Then (see (A6)):

$$H_c = \frac{1}{4} (m_s/\chi_{\perp}) [4 \chi_{\perp} (Aq_0^2 - |K|/2) / m_s^2 - 1],$$

where it was taken into account that K is negative. It appears from this expression that H_c is a decreasing function of $|K|$, as can be expected from simple energetic considerations. This holds for any orientation of the applied field. Experimentally, the low field slope $2/3\chi_{\perp}$ is seen to increase slightly with La doping, yielding χ_{\perp} values between 7.5×10^{-5} for pure BiFeO_3 and 10.0×10^{-5} for $x=0.125$ (See Table 1). While we have no explanation as to the reason for this increase, we have included it in our calculation. We find that increasing the anisotropy density K shifts the transition region towards lower fields. Figure 4 represents the $m(H)$ curves computed for

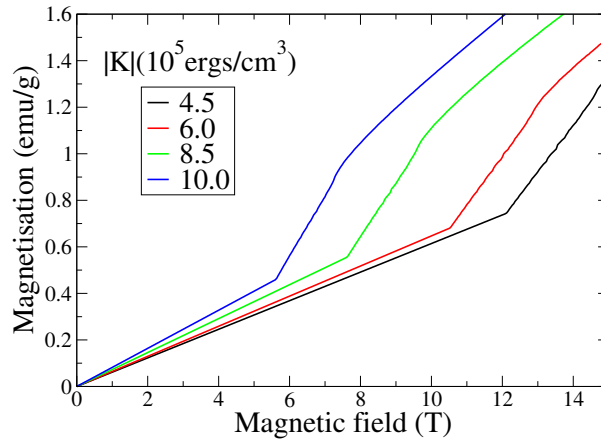


Figure 4: Calculated $m(H)$ curves for a ceramic sample for different values of the anisotropy density, showing the transition between the spiral magnetic state at low fields towards a collinear AF state at high field.

different values of $|K|$, with an energy gain for the spiral state²² $E_s = Aq_0^2 = 6.5 \times 10^5$ ergs/cm³ and a weak ferromagnetic magnetisation $m_s = 1.2$ emu/cm³ = 0.15 emu/g (using the specific mass $\rho = 8.33$ g/cm³ of BiFeO₃). These curves, although not matching precisely the experimental data, reproduce qualitatively the observed features for $x \leq 0.15$ and put on a more solid ground the assumption of an increasing anisotropy density with increasing La content in the rhombohedral Bi_{1-x}La_xFeO₃ compounds.

The presence of a small remanent magnetisation, even in samples with $x=0.05$ and 0.10, could be due to the fact that, when increasing the field up to 14T, a certain amount of crystallites with the correct orientation undergo the transition towards a collinear state, thus acquiring a small ferromagnetic magnetisation which is therefore subject to hysteresis.

For $x > 0.15$, the magnetisation is approximately linear with field and a weak ferromagnetic component is observed when extrapolating the $m(H)$ curve to $H=0$. In order to

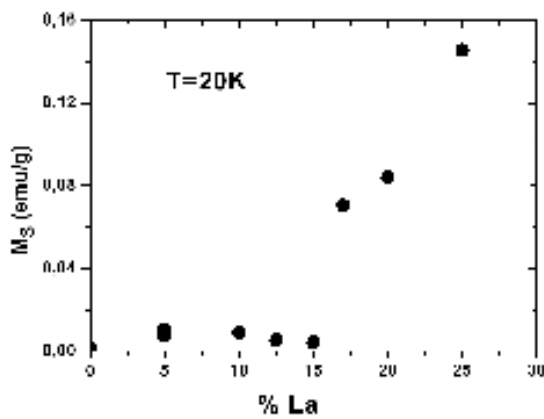


Figure 5 : Spontaneous magnetization in zero field in the Bi_{1-x}La_xFeO₃ series at 20K.

check this behaviour, we measured the spontaneous magnetization M_s^0 in zero field after cooling the sample in a very low residual field $H_{res} < 2G$ as a function of the La content (Figure 5). For $x < 0.17$, there is no spontaneous magnetization, the spiral spin structure being present in zero field. For $x \geq 0.17$, a non-zero spontaneous moment arises, showing that the spatially modulated magnetic structure has probably disappeared. This result is in good agreement with the ⁵⁷Fe NMR studies¹⁸ which have shown that the cycloid is destroyed for a La concentration between 0.1 and 0.2. According to the X-ray diffraction results, this corresponds to the transformation from a rhombohedral to an orthorhombic crystal structure. The presence of a small spontaneous magnetisation could be an indication that the magnetic structure in the orthorhombic phase is a canted AF one.

2) Magnetodielectric measurements

In Figure 6a is reported the magnetic field dependence of the normalized dielectric constant $\epsilon(H)/\epsilon(H=0)$ of samples with different La contents $0 < x \leq 0.25$ at 100K.

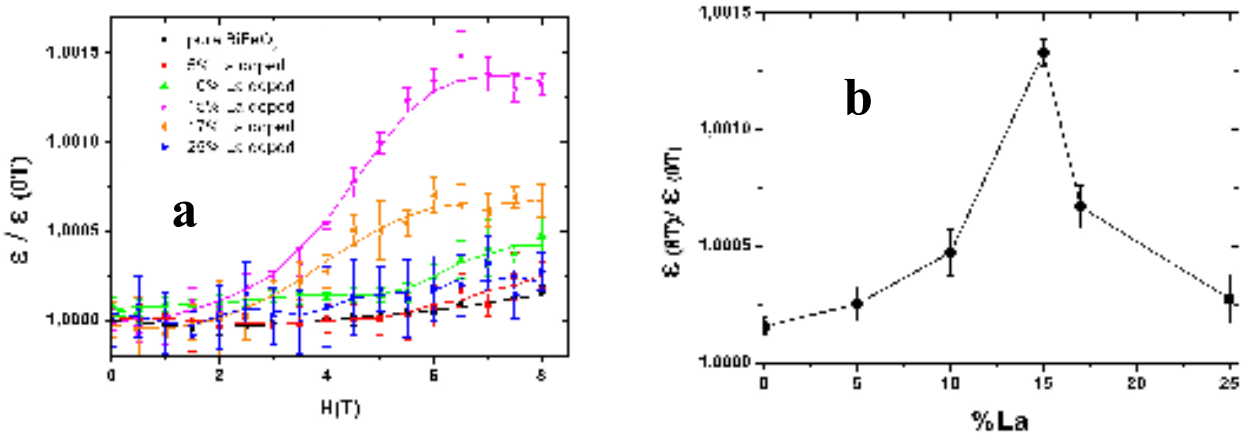


Figure 6: *a)* Magnetic field dependence of the normalized dielectric constant in the $\text{Bi}_{1-x}\text{La}_x\text{FeO}_3$ series at 100K; *b)* Dependence on La content of the 8T value of the normalized dielectric constant.

The ceramic pellets for these measurements have been made with powders extracted from the same batches as those used for the magnetic measurements. In pure BiFeO_3 , as well as for $x=0.05$, there is no clearcut field dependence of the dielectric constant up to 8T. For $x=0.10$, a slight increase of ϵ above 5T is observed, and for $x=0.15$ a clear upturn occurs above 3T, culminating in a 0.14% relative enhancement around 8T. On further increasing the La content, the field dependence progressively disappears (see Figure 6b). We associate the stronger field dependence of ϵ as x increases up to 0.15 to the destruction of the spiral spin structure at lower fields, as shown by the preceding magnetisation data. Figure 7 shows the comparison of the experimentally determined threshold fields for deviation of the $m(H)$ curves from a linear law and for deviation of the $\epsilon(H)$ curves from a constant value, as a function of La content. The correlation is obvious, which is a strong indication that the two phenomena are linked. In the following, we interpret the behaviour of $\epsilon(H)$ in a way similar to the cancellation of the linear magnetoelectric effect by the spiral magnetic structure and its recovery in the presence of a strong magnetic field.

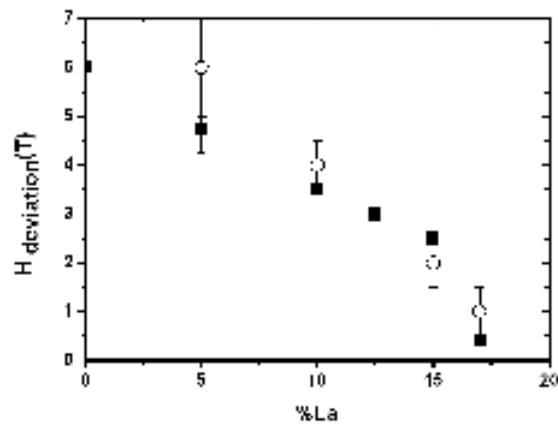


Figure 7: Threshold fields for deviation of $m(H)$ from a linear law (full squares) and for deviation of $\epsilon(H)$ from a constant (open circles) in the $\text{Bi}_{1-x}\text{La}_x\text{FeO}_3$ for $x < 0.17$.

In the presence of magnetic and electric fields, the Landau free energy for a multiferroic material reads, up to the second order in the fields (and using the Einstein rule of summation over repeated indices):

$$-g(E, H; T) = {}^S P_i E_i + {}^S J_i H_i + \frac{1}{2} \varepsilon_0 \varepsilon_{ik} E_i E_k + \frac{1}{2} \mu_0 \mu_{ik} H_i H_k + \alpha_{ik} E_i H_k + \frac{1}{2} \beta_{ijk} E_i H_j H_k + \frac{1}{2} \gamma_{ijk} H_i E_j E_k$$

where ${}^S P$ and ${}^S J$ are respectively the spontaneous electric polarisation and magnetisation, ε_0 and μ_0 the free space permittivity and permeability, and the second rank tensors ε_{ik} , μ_{ik} and α_{ik} the relative permittivity, permeability and the linear magnetoelectric coupling respectively (for a review see Ref. 23). The third rank tensors β_{ijk} and γ_{ijk} are associated with higher order magnetoelectric interactions^{24,25}. The k -component of the electric polarisation is then:

$$P_k(E, H; T) = -\frac{\partial g}{\partial E_k} = {}^S P_k + \varepsilon_0 \varepsilon_{ik} E_i + \alpha_{ki} H_i + \frac{1}{2} \beta_{kij} H_i H_j + \gamma_{ijk} H_i E_j, \quad (10)$$

In the spiral AF phase of BiFeO₃, the magnetoelectric tensor α can be derived from energy invariants containing terms of the type $E_i H_k L_j$, i.e. it depends linearly on the AF vector \mathbf{L} . Since the average $\langle \mathbf{L} \rangle$ of the AF vector over a period of the spiral is zero, so is $\langle \alpha \rangle$, resulting in the absence of any H-linear dependence of \mathbf{P} (no linear magnetoelectric effect). Both tensors β_{ijk} and γ_{ijk} should be non-zero in BiFeO₃ since the crystal structure is not invariant by space inversion ($\beta_{ijk} \neq 0$) and the magnetic structure is not invariant by time inversion ($\gamma_{ijk} \neq 0$). In our ac measurement of the dielectric constant (or of the relative permittivity), the magnetic field \mathbf{H} is static and the electric field \mathbf{E} is oscillating. Therefore, in order to obtain the ac induced polarisation, we must keep only the terms proportional to \mathbf{E} in the expression for \mathbf{P} . Then, the H-dependent renormalised permittivity tensor writes:

$$\varepsilon_0 \Sigma_{ij}(\mathbf{H}) = \varepsilon_0 \varepsilon_{ij} + \frac{1}{2} \gamma_{kij} H_k, \quad (11)$$

i.e. it depends linearly on the high order magnetoelectric tensor γ which, in a way similar to the α tensor, can be derived from energy invariants of the type $H_i E_j E_k L_m$ and thus also depends linearly on the AF vector \mathbf{L} . In the spiral magnetic phase of pure BiFeO₃, $\langle \gamma \rangle = 0$ and there is no linear H-dependence of the dielectric constant, as experimentally observed. On increasing the La content, the spiral structure is progressively destroyed in lower fields, leading to a measurable H-dependence of the dielectric constant. Averaging over the orientations in our ceramic sample should not alter the main conclusions derived from expression (11), which provides thus a qualitative explanation of the observed behaviour of $\varepsilon(H)$.

x (La doping)	$\chi_{\perp} \times 10^5$ (low field)	$M_{\text{rem}} \times 10^2$ (emu/g)	$M_s \times 10^2$ (emu/g)	$\varepsilon_{8T} / \varepsilon_{0T}$
0	7.654 ± 0.013	0	0.102 ± 0.048	$1.00016 \pm 3.710E-5$
0.05	7.888 ± 0.064	1.406 ± 0.020	0.741 ± 0.017	$1.00025 \pm 7.271E-5$
0.10	9.246 ± 0.030	2.366 ± 0.011	0.896 ± 0.016	$1.00047 \pm 9.926E-5$
0.125	10.318 ± 0.061	3.912 ± 0.013	0.537 ± 0.012	-
0.15	11.942 ± 0.512	7.030 ± 0.007	0.412 ± 0.547	$1.00133 \pm 5.969E-5$
0.17	12.360 ± 0.398	9.371 ± 0.013	7.056 ± 0.266	$1.00067 \pm 9.192E-5$

Table 1: overall view of the magnetic and dielectric parameters as a function of the La-doping of $\text{Bi}_{1-x}\text{La}_x\text{FeO}_3$, extracted from the figures.

DISCUSSION

We considered here only a negative sign for the anisotropy constant K , in line with our assumption that the magnetic moments in the high field collinear phase lie in the basal plane

xOy. We tried other reasonable configurations, but, in this approximate model, none of them yield a solution for the critical field for all orientations in the crystal axes. The sign of the constant K is irrelevant as to the stability of the spiral structure as long as the condition:

$-Aq_0^2 + |K|/2 < 0$ is fulfilled, i.e. the spiral structure is stable if $|K| < 2Aq_0^2$, which holds for our calculations. Our second assumption about the collinear spin configuration, i.e. that \mathbf{L} orients itself perpendicular to \mathbf{H} implies that the powder susceptibility in the high field phase is χ_{\perp} (see expression (8)). The comparison with experimental results shows that this slope is over-estimated, which could be due to the crudeness of the above assumption. Neutron scattering with a magnetic field could help determine the high field magnetic structure if large enough crystals of the doped materials were available.

The magnetic and dielectric properties of the $x=0.15$ compound have recently been studied in Ref.26. In their sample, the authors find a crystal structure very close to orthorhombic, without rhombohedral distortion, in contradiction with our findings. Nevertheless, they obtain a weak remanent magnetisation after a field loop up to 6T, with the same M_{rem} value as ours (0.075emu.g). We think that these results could be caused by the fact that $x=0.15$ is a borderline composition. Small deviations from this nominal value can push the material on one or either side of the rhomboedral to orthorhombic transition, but the spiral and collinear magnetic structures respectively at low and high field would remain unchanged, thus yielding the same magnetic response as in our sample.

CONCLUSION

In this investigation, we have performed magnetic and dielectric measurements as a function of magnetic field in La-doped BiFeO_3 polycrystalline samples. We have shown that La substitution reduces the transition field from the spatially modulated to the homogeneous magnetic state and that there is a good correlation between the values found by magnetic and dielectric measurements for this transition field as a function of doping. We have shown that the transition is broadened for polycrystalline samples, due to the orientational dependence of this critical field, and that the latter is a decreasing function of the anisotropy energy density. Moreover, it has been shown by neutron powder diffraction²⁷ that Mn doping in BiFeO_3 increases the periodicity λ of the long range spiral spin modulation. It should be of a great interest to understand how to link the rare earth doping, λ and the magnetic anisotropy.

In the sample $\text{Bi}_{0.85}\text{La}_{0.15}\text{FeO}_3$, which has the rhombohedral structure, we obtain the minimum field (7-8T) for complete transition to the collinear AF phase and the maximum positive magnetocapacitance effect at 8T.

Acknowledgements

We acknowledge A.K.Zvezdin. for fruitful discussions.

This work was supported by NTOS-1-45147 ‘‘FEMMES’’.

APPENDIX

Our calculation follows the formalism developed in Ref.1. It uses a simplified model to obtain the critical field for transition from the spiral magnetic phase to the collinear AF phase for an arbitrary orientation (ψ, γ) of the applied field \mathbf{H} , in the frame defined in Fig.2. Whereas it is known that the cycloidal spiral is harmonic (i.e. sine-wave) at room temperature and in zero field, some anharmonicity sets in on lowering the temperature and/or on increasing the magnetic field. We shall neglect here these departures from the sine-wave cycloid. Apart from the exchange, anisotropy and Zeeman terms in the energy, we write the ME coupling as an effective Zeeman energy with a field $\mathbf{H}_{\text{ME}} = \beta \mathbf{L} \times \mathbf{P}^0$, which adds to the applied field. In the spiral phase, the exchange energy density gain over the collinear phase is $E_s = Aq_0^2$. The anisotropy energy density is $E_a = K \sin^2 \theta$, where θ is the polar angle of \mathbf{L} . Averaging over a

period, in the harmonic approximation for the cycloid, yields $\langle E_a \rangle = 1/2 K$. In the collinear phase, our assumption is that the \mathbf{L} vector remains in the xOy plane ($\theta = \pi/2$), which implies $K < 0$, and is perpendicular to \mathbf{H} ; hence $\mathbf{L} = (-\sin\gamma, \cos\gamma, 0)$ and $E_a = -|K|$. The Zeeman energy is written: $E_Z = -1/2 \chi_{\perp} H_{\perp}^2$, where H_{\perp} is the component of the total field $\mathbf{H} + \mathbf{H}_{ME}$ perpendicular to \mathbf{L} (we neglect χ_{\parallel} as $T \ll T_N$). Introducing the peak ME-induced magnetisation along Ox in the spiral phase m_s , then: $m_s = \chi_{\perp} H_{ME} = \chi_{\perp} \beta P^0$, whence the ME coupling parameter β is worth: $\beta P^0 = m_s / \chi_{\perp}$. After a straightforward calculation, one obtains the energy in the spiral phase (after averaging over a period):

$$E_{SP} = -Aq_0^2 - 1/2 |K| - 1/4 \chi_{\perp} H^2 (1 + \sin^2 \psi \cos^2 \gamma) - 1/4 \chi_{\perp} (m_s / \chi_{\perp})^2 \quad (\text{A1})$$

and the magnetisation:

$$M_{SP} = 1/2 \chi_{\perp} H (1 + \sin^2 \psi \cos^2 \gamma); \quad (\text{A2})$$

in the collinear AF phase, the energy is:

$$E_{AF} = -|K| - 1/2 \chi_{\perp} H^2 - 1/2 \chi_{\perp} (m_s / \chi_{\perp})^2 - m_s H \sin \psi \quad (\text{A3})$$

with the magnetisation:

$$M_{AF} = \chi_{\perp} H + m_s \sin \psi. \quad (\text{A4})$$

With reasonable values of the parameters, E_{SP} is lower than E_{AS} at low fields, thus above the critical field H_c the collinear phase becomes the ground state. The second order equation that yields the critical field is:

$$(1 - \sin^2 \psi \cos^2 \gamma) H_c^2 + 4(m_s / \chi_{\perp}) H_c \sin \psi + (m_s / \chi_{\perp})^2 - 4 / \chi_{\perp} (Aq_0^2 - |K|/2) = 0. \quad (\text{A5})$$

If $\psi = \pi/2$ and $\gamma = 0$ or π (i.e. \mathbf{H} is along the x-axis), the equation is first order and the critical field writes:

$$H_c(\pi/2, 0 \text{ or } \pi) = 1/4 (m_s / \chi_{\perp}) [4 \chi_{\perp} (Aq_0^2 - |K|/2) / m_s^2 - 1]. \quad (\text{A6})$$

For an orientation of H outside the x-axis, the solution for H_c is:

$$H_c(\psi, \theta) = 2 (m_s / \chi_{\perp}) \sin \psi / (1 - \sin^2 \psi \cos^2 \gamma) (\sqrt{N} - 1), \quad (\text{A7})$$

$$\text{where } N = 1 - (1 - \sin^2 \psi \cos^2 \gamma) / (4 \sin^2 \psi) [1 - 4 \chi_{\perp} (Aq_0^2 - |K|/2) / m_s^2]. \quad (\text{A8})$$

References

- ¹ See for instance A.Kadomtseva, A. Zvezdin, Y. Popov, A. Pyatakov, and G. Vorob'ev, JETP Lett. **79**, 571 (2004) and references therein.
- ² A. K. Zvezdin, A. P. Pyatakov, Conferences and symposia Physics-Uspekhi **47**, 416 (2004)
- ³ Manfred Fiebig 2005 *J. Phys. D: Appl. Phys.* **38** R123
- ⁴ G. A. Smolenskii and I. Chupis, [Sov. Phys. Usp. **25**, 475 \(1982\)](#)
- ⁵ W. Eerenstein, N. D. Mathur, and J. F. Scott, [Nature \(London\) **442**, 759 \(2006\)](#).
[\[MEDLINE\]](#)
- ⁶ I. Sosnowska, T. Peterlin-Neumaier, and E. Steichele, J. Phys. C **15**, 4835 (1982).
- ⁷ I. Sosnowska, M. Loewenhaupt, W. I. F. David, and R. Ibberson, [Physica B **180&181**, 117 \(1992\)](#).
- ⁸ Yu. F. Popov, A. K. Zvezdin, G. P. Vorob'ev, A. M. Kadomtseva, V. A. Murashev, and D. N. Rakov, JETP Lett. **57**, 69 (1993)
- ⁹ D. Lebeugle, D. Colson, A. Forget, M. Viret, A. M. Bataille and A. Gukasov, Phys. Rev. Lett. **100**, 227602 (2008)
- ¹⁰ Yu.F. Popov, A.M. Kadomtseva, A.K. Zvezdin, G.P. Vorob'ev, and A.P. Pyatakov, in *Magneto-electronic Phenomena in Crystals*, edited by Manfred Fiebig (Kluwer Academic Publishers, Dordrecht, 2004).
- ¹¹ Y. H. Chu *et al*, Nature Materials **7**, 478 (2008).

-
- ¹² G. P. Vorob'ev, A. K. Zvezdin, A. M. Kadomtseva, Yu. F. Popov, V. A. Murashov, and Yu. P. Chernenkov, *Phys. Solid State* **37**, 1329 (1995)
- ¹³ Sosnowska, I.; Przenioslo, R.; Fischer, P.; Murashov, V. A, *Journal of Magnetism and Magnetic Materials* (1996), 160(International Conference on Soft Magnetic Materials, 1995).
- ¹⁴ J. R. Sahu, C. N. R. Rao, *Solid State Sciences* **9**, 950 (2007)
- ¹⁵ Y-H. Lin, Q. Jiang, Y. Wang, C-W. Nan, L. Chen, J. Yu, *Appl. Phys. Lett.* **90**, 172507 (2007).
- ¹⁶ Z. X. Cheng, A. H. Li, X. L. Wang, S. X. Dou, K. Ozawa, H. Kimura, S. J. Zhang and T. R. ShROUT, *J. of Appl. Phys.* **103** 07E507 (2008)
- ¹⁷ S. T. Zhang, L. Pang, Y. Zhang, M. Lu and Y. Chen *J. of Appl. Phys.* **100** 114108 (2006)
- ¹⁸ A. V. Zalesskii, A. A. Frolov, T. A. Khimich, and A. A. Bush, *Phys. Solid State* **45**, 141 (2003).
- ¹⁹ I. E. Dzyaloshinskii, *Sov. Phys. JETP* **5**, 1259 (1957)
- ²⁰ T. Moriya, *Phys. Rev.* **120**, 91 (1960)
- ²¹ D. Lebeugle, D. Colson, A. Forget, M. Viret, P. Bonville, J. F. Marucco, and S. Fusil, *Phys. Rev. B* **76**, 024116 (2007).
- ²² B. Ruetter, S. Zvyagin, A. P. Pyatakov, A. Bush, J. F. Li, V. I. Belotelov, A. K. Zvezdin, and D. Viehland, *Phys. Rev. B* **69**, 064114 (2004)
- ²³ H. Schmid, in *Introduction to Complex Medium for Optics and Electromagnetics*, Eds W.S. Weiglhofer and A. Lakhtakia, SPIE Press, USA, 167-195 (2003)
- ²⁴ E. Ascher, *Phil Mag.* **17**, 149 (1968)
- ²⁵ H. Grimmer, *Ferroelectrics* **161**, 181 (1994),
- ²⁶ G. L. Yuan, K. Z. Baba-Kishi, J. -M. Liu, S. W. Or, Y. P. Wang and Z. G. Liu, *J. Am. Ceram. Soc.* **89**, 3136 (2006)
- ²⁷ I. Sosnowska, W. Schäfer, W. Kockelmann, K. H. Andersen and I. O. Troyanchuk, *Applied Physics A* **74** [Suppl.], S1040-S1042 (2002)